Jun 2004 CHINESE JOURNAL OF ENGINEERING MATHEMATICS Vol 21 No 3

Article ID:1005-3085(2004)03-0285-22

# Free Boundary Problems in the Steel Industry

A.D Fitt[1], J.R. Ockendon[2], C.P.Please[1]

(1- School of Mathematics, University of Southampton, Highfield, Southampton SO17 1BJ UK;
2- OCIAM, Mathematical Institute, 24–29 St. Giles, Oxford, OX1 3LB)

**Abstract:** This paper considers two novel free boundary problems that emerge from modelling processes basic to steel manufacture. The first process concerns the spray cooling of hot steel sheet during the process of continuous casting. Here, an important practical consideration is the non-monotonicity of the measured heat transfer from the steel as a function of the steel temperature. In order to understand this phenomenon, a two-phase flow model is written down for the heating and vapourisation of the water spray. This model relies on a microscale analysis of droplet vapourisation and, in a steady state, it reduces to a coupled system of nonlinear ordinary differential equations for the spray temperature and water content. This system predicts the conditions for the existence or otherwise of a free boundary separating the two-phase region from a dry vapour layer close to the steel plate. The thickness of this vapour layer is determined by the solution of a generalised Stefan problem. The second process concerns the macroscopic modelling of pig iron production in blast furnaces. In the simplest scenario, the blast furnace may be roughly divided into a porous solid region overlaying a hot high pressure gaseous zone. The gas reacts with the solid in a thin "intermediate region" at the base of the solid region and it is in this intermediate region that the pig iron is produced. A free boundary model is proposed for the location of the intermediate region and its stability is investigated.

**Keywords:** free boundary problem; mathematical modelling; stability

**Classification:** AMS(2000) 58J35 **CLC number:** O175.2 **Document code:** A

## 1 Introduction

The aim of this paper is to describe some simple mathematical modelling and analysis that can help to understand the functioning of two processes fundamental to steel manufacture. Both processes concern the spatial inhomogeneity of macroscopic heat and mass transfer. The first is motivated by the need to quantify the effectiveness of the spray cooling of hot steel sheet, where the existence or otherwise of a dry vapour layer near the sheet is vital; the second concerns the morphology of the solids in a blast furnace, where the location and stability of the reactive layer in which the pig iron is produced is vital.

Although the paper is divided into distinct halves, each with its own more detailed introduction and conclusions, the same basic mathematical methodology is used throughout; this comprises modelling, nondimensionalisation, asymptotic and numerical analysis and a discussion of the physical applicability of the predictions.

Received date: 2003-08-20

## 2 Spray Cooling

### 2.1 Physical background

The simplest scenario for the cooling of hot steel sheet by water sprays during continuous casting is to assume that the spray consists of a large number of water droplets that are projected normally towards the steel surface and that all the relevant physical variables depend only on time and distance from the steel surface.

The main purpose of this investigation is to explain the qualitative results of Figure 1, where the measured heat transfer $Q$ from the steel is plotted against the surface steel temperature. One might expect that, for a constant rate of spraying, as the steel temperature increased so the heat transfer from the steel would increase. However, Figure 1 shows that this is not the case. Moreover for strong sprays, droplets of water can clearly be seen "running off" the hot steel. Let us therefore consider two extreme scenarios for the way in which the heat transfer is affected by the spraying rate:

- For low spraying rates, the heat transfer from the steel is sufficiently large that all water droplets are vapourised before they reach the surface of the hot steel. This means that the steel is surrounded by a "vapour blanket" much thicker than a typical droplet size. Obviously this is a non-optimal condition as far as the cooling of the steel is concerned, because this blanket acts as an insulator for the hot steel.
- For high spraying rates, many droplets arrive at the surface of the steel without having vapourised. Once such droplets impact the steel,

The "Leidenfrost effect"[3] allows the droplets (a) to remain intact for longer than might be expected, owing to the insulating vapour blanket that is formed at the interface between an individual droplet and the hot steel and (b) to move across the steel in a virtually friction-free manner.

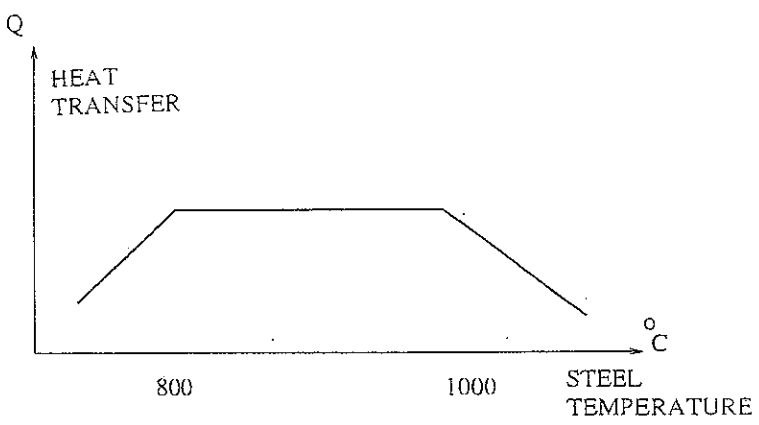


Figure 1: *Heat transfer $Q$ as a function of steel temperature for steel cooling at a constant spray rate*

We can now propose that the non-monotonicity in Figure 1 is related to the existence of an optimal regime that prevails when the droplets arrive at the surface of the steel just as their radius drops to zero; when the steel temperature is too high for the prescribed spray rate, the first of the above scenarios is operating, and when it is too low the second scenario takes over. Hence, one of the major outputs of the model that we seek to develop below will be to predict the conditions under which optimal vapourisation can occur.

### 2.2 Mathematical modelling of the water spray

We now propose a simple two-phase flow model for the flow and vapourisation of water drops in the vicinity of hot steel. The model is based on the "ensemble averaging" two-phase flow methodology outlined in [1]. For simplicity we only consider flow in one space dimension $x$, which is normal to the steel surface, and assume that there are two phases only: the droplets (dispersed phase) and the vapour (continuous phase). It is realistic to assume that the vapour is incompressible, and thus the equations that govern the unidirectional flow are

$$(\rho_d\alpha)_t + (\rho_d\alpha u)_x = -f, \tag{1}$$

$$(\rho_g(1-\alpha))_t + (\rho_g(1-\alpha)v)_x = f, \tag{2}$$

$$(\rho_d\alpha u)_t + (\rho_d\alpha u^2)_x = -\Phi - uf, \tag{3}$$

$$(\rho_g(1-\alpha)v)_t + (\rho_g(1-\alpha)v^2)_x + p_{gx} = \Phi + uf, \tag{4}$$

$$\rho_d c_p((\alpha T)_t + (\alpha u T)_x) = kT_{xx} + E, \tag{5}$$

$$\rho_g c_{pg}(((1-\alpha)T_g)_t + ((1-\alpha)vT_g)_x) = k_g T_{gxx} - E. \tag{6}$$

In (1)–(6) the notation is as follows: $t$ denotes time, $\rho_d$ and $\rho_g$ denote the density of the droplets and the vapour respectively, $\alpha$ denotes the void fraction of droplets ($0 \leq \alpha \leq 1$ - when $\alpha = 0$ there are no drops), $u$ and $v$ denote the respective speeds of the droplets and the vapour, $p_g$ denotes the pressure in the vapour phase and the droplet and gas temperatures are given by $T$ and $T_g$. $T_V$ denotes the temperature of vapourisation of the fluid in the droplets. The thermal conductivity and specific heat are denoted by $k$ and $c_p$ respectively, a subscript $g$ denoting properties in the gas. All such thermal properties are assumed to be constant (see Appendix 1 for typical values). The two-phase flow problem is driven by the source terms $f$, $\Phi$ and $E$. The right-hand sides of (1) and (2) characterise the mass that is transferred from the droplets to the vapour as a droplet vapourises, with $f$ denoting the mass per second per unit volume that is transferred. At present, $f$ is unknown and needs to be specified using a submodel. The term $\Phi$ accounts for the viscous drag experienced by the droplets as they move through the gas. We assume henceforth that, since a source has no drag in a slow flow, standard drag models may be used and it is not necessary to pursue the fact that the droplets are vapourising. $E$ denotes the distributed energy sources and sinks that affect the gas and the droplet flow. We also note that, if the number density (number per unit volume) of droplets in the flow is denoted by $N$, then

$$\frac{4}{3}\pi s^3 N = \alpha, \tag{7}$$

where $s$ is the average droplet radius.

It should be noted that a number of common two-phase flow assumptions have been made in deriving the governing equations (1)–(6). In particular:

- we have followed [1] in dealing with products of averages;
- all sources of drag in the momentum equations have been lumped together via a single drag term $\Phi$;
- the standard "dusty gas" two-phase flow hypothesis (see, for example [1]) has been invoked in order to set the "pressure" in the drops equal to a constant

We now consider the extra information that we need to close the equations (1)–(6). First, we note that the mass transfer term is given by

$$f = -4\pi\rho_d s^2 \dot{s} N, \tag{8}$$

since there are $N$ droplets each of density $\rho_d$, the surface area of each of which is $4\pi s^2$, and the surface recedes at a rate $\dot{s}$; of course, a submodel to determine $\dot{s}$ is still required if (8) is to be of any use.

Determining an accurate form for the drag, $\Phi$, is not a simple matter as the averaging involved has to be carried out rather carefully. In [4], it was found that, for the disperse low Reynolds number flows relevant to spray cooling,

$$\Phi = \frac{9\alpha\mu_g}{2s^2}(u - v),$$

where $\mu_g$ denotes the dynamic viscosity of the gas.

One of the governing equations (1)–(6) may be dealt with at once. We observe that the conduction time scale $\tau_c$ in a drop of radius $s_0$ is given according to the values in the Appendix 1 by

$$\tau_c = \frac{s_0^2 \rho_d c_p}{k} \sim 6 \times 10^{-4}\text{sec}.$$

This suggests that a drop travelling a typical distance of 1m at a speed of 5m/s takes only about three thousandths of its total travel time to heat up by conduction in the drop. We conclude that sensible heating of a drop is thus virtually instantaneous and the vapourisation process is controlled completely by latent heat. The temperature in a droplet is thus essentially constant and so, from (5), we have $E = -fc_pT_V$.

### 2.3 Drop vapourisation

The two-phase flow model presented in section 2.2 cannot be analysed until a suitable submodel has been proposed for the vapourisation of an individual droplet so that the mass source term $f$ can be determined. We therefore consider the local problem close to a single droplet. Since the temperature in a droplet is effectively constant, the details of the drop vapourisation are determined entirely by a local Stefan problem in the gas. We assume that the local problem is spherically symmetric and that the the velocity of the gas produced by the vapourising droplet liquid relative to the centre of the droplet is given by $v_{gl}$. We denote by $r$ the distance from the centre of a droplet and assume that the droplet (which has initial radius $s_0$) has radius $s(t)$ at time $t$. Conservation of mass for the gas then yields

$$\frac{1}{r^2}(r^2 v_{gl})_r = 0.$$

The *local* gas temperature $T(r,t)$ satisfies

$$\frac{k_g}{r^2}(r^2 T_r)_r = \rho_g c_{pg}(T_t + v_{gl}T_r), \tag{9}$$

where we will soon see that the right-hand side may be neglected, with

$$T \to T_g(x,t) \text{ as } r \to \infty, \qquad T = T_V \text{ at } r = s(t)$$

The specification of the local problem is completed by supplying a boundary condition for $v_{gl}$ at the vapourisation front $s(t)$ and a Stefan condition to allow the free boundary $s(t)$ to be determined. To derive the former, suppose that the free boundary $r = s(t)$ moves in a time $dt$ to $r = s(t + dt)$ Then the amount of droplet liquid that is gasified is $\rho_d[s(t + dt) - s(t)]$. Since at the free boundary the gas moves away with a radial speed $v_{gl} + \dot{s}$, mass conservation dictates that

$$v_{gl} = \left(\frac{\rho_g - \rho_d}{\rho_g}\right)\dot{s} \text{ at } r = s(t). \tag{10}$$

Since in the current case of interest $\rho_d \gg \rho_g$, we immediately approximate (10) by

$$v_{gl} = -\frac{\rho_d}{\rho_g}\dot{s} \text{ at } r = s(t).$$

The Stefan condition is, as usual, given by

$$-\rho_d L\dot{s} = k_g T_r \tag{11}$$

where $L$ denotes the latent heat of vapourisation of the fluid in a droplet, and use has been made of the fact that, by our earlier arguments, the temperature gradient within the drop is zero.

It is apparent from (11) that the time scale for droplet evaporation is of $O(\rho_d L s_0^2/k_g(T_g - T_V))$ which, for the values given in the Appendix 1, greatly exceeds $\tau_c$, as expected. Moreover, the right-hand side of (9) is of $O(c_{pg}(T_g - T_V)/L) = \gamma$, say, relative to the left-hand side. This parameter is small, and this justifies our use of the quasi-steady solution

$$v_{gl} = -\frac{\rho_d s^2\dot{s}}{\rho_g r^2}, \quad T = T_V + \rho_d\frac{Ls^2\dot{s}}{k_g}\left(\frac{1}{r} - \frac{1}{s}\right).$$

Hence, from (9), following an individual droplet the radius evolves according to

$$\dot{s} = -\frac{k_g(T_g(x,t) - T_V)}{s\rho_d L} \tag{12}$$

### 2.4 Steady-state analysis

Now that a submodel has been proposed for $\dot{s}$, we are in a position to analyse the equations of motion (1)–(6) Start-up or wind-down processes could of course be considered by adopting a numerical approach to (1)–(6), but here we will only consider the steady state in which all the time derivatives in (1)–(6) are zero and $\dot{s}$ in (12) is replaced by the convective derivative $us_x$.

In addition we ignore equations (4) and (5) on the grounds that the former serves only to provide an equation for the gas pressure (which could be calculated, if desired, once all the other variables have been determined) and, as already noted, the latter simply states that the temperature in a droplet is constant. We therefore study the ordinary differential equations

$$(\rho_d\alpha u)_x = -f, \tag{13}$$

$$(\rho_g(1 - \alpha)v)_x = f, \tag{14}$$

$$(\rho_d \alpha u^2)_x = -\frac{9\alpha\mu_g(u-v)}{2s^2} - uf, \tag{15}$$

$$us_x = -\frac{k_g}{s\rho_d L}(T_g(x,t) - T_V), \tag{16}$$

$$\rho_g c_{pg}((1-\alpha)vT_g)_x = k_g T_{gxx} + f c_{pg} T_V, \tag{17}$$

where, using (7), (8) and (12),

$$f = \frac{3\alpha k_g}{s^2 L}(T_g(x,t) - T_V).$$

The equations are to be solved in the region $0 \le x \le D$ where $x = 0$ denotes the spray jet orifices and $x = D$ the surface of the steel. A number of different specifications of boundary conditions are possible, but for the present we assume that the properties of the water spray are known at $x = 0$, the temperature gradient is zero there, and at $x = D$ the gas has the same temperature as the steel and no gas can pass through the steel. Thus

$$T_{gx}(0) = 0, \quad s(0) = s_0, \quad \alpha(0) = \alpha_0, \quad u(0) = U$$

and

$$v(D) = 0, \quad T_g(D) = T_s,$$

where $T_s$ denotes the steel temperature, $\alpha_0$ and $s_0$ denote respectively the initial void fraction and drop radius, and $U$ denotes the droplet speed at the spray nozzle exit.

We can now non-dimensionalise the the model according to

$$T_g = T_V + \bar{\theta}(T_s - T_V), \quad \alpha = \alpha_0\bar{\alpha}, \quad s = s_0\bar{s}, \quad u = U\bar{u}, \quad v = \frac{U\rho_d\alpha_0}{\rho_g}\bar{v}, \quad x = D\bar{x}.$$

This choice of scalings reflects the fact that the scale for the gas velocity $v$ is effectively determined by (14), and that the gas temperature must at all times be between $T_V$ and $T_s$. Also, we will consider only disperse sprays where $\alpha_0 \ll 1$ so that we may approximate $1-\alpha$ by 1. In non-dimensional form, the equations (13)–(17) become

$$(\bar{\alpha}\bar{u})_{\bar{x}} = -M\frac{\bar{\theta}\bar{\alpha}}{\bar{s}^2}, \tag{18}$$

$$(\bar{v})_{\bar{x}} = M\frac{\bar{\theta}\bar{\alpha}}{\bar{s}^2}, \tag{19}$$

$$(\bar{\alpha}\bar{u}^2)_{\bar{x}} = -\frac{9N\bar{\alpha}}{2\bar{s}^2}(\lambda\bar{u} - \bar{v}) - M\frac{\bar{u}\bar{\alpha}\bar{\theta}}{\bar{s}^2}, \tag{20}$$

$$\bar{u}\bar{s}_{\bar{x}} = -M\frac{\bar{\theta}}{3\bar{s}}, \tag{21}$$

$$(\bar{v}\bar{\theta})_{\bar{x}} = \Gamma\bar{\theta}_{\bar{x}\bar{x}} + RM\frac{\bar{\alpha}\bar{\theta}}{\bar{s}^2}, \tag{22}$$

where the key non-dimensional parameters are given by

$$M = \frac{3Dk_g(T_s - T_V)}{U\rho_d L s_0^2}, \quad \Gamma = \frac{k_g}{c_{pg}\rho_d\alpha_0 UD}, \quad N = \frac{\mu_g D\alpha_0}{U\rho_g s_0^2},$$

$$\lambda = \frac{\rho_g}{\rho_d\alpha_0}, \quad R = \frac{T_V}{T_s - T_V},$$

and the boundary conditions are

$$\bar{\theta}(1) = 1, \quad \bar{v}(1) = 0, \quad \bar{\theta}'(0) = 0, \quad \bar{s}(0) = 1, \quad \bar{\alpha}(0) = 1, \quad \bar{u}(0) = 1.$$

We now drop the bars from the variables for simplicity. The system may be reduced in order by noting that, from (18)and(19)

$$\alpha u + v = \text{constant} = c_1,$$

say, and, from (18) and (20) that

$$\alpha u u = -\frac{9N\alpha}{2s^2}(\lambda u - v)$$

where $' = d/dx$. Hence, writing $\alpha u = w$, we find that

$$w' = -\frac{Mw\theta}{us^2}, \tag{23}$$

$$u' = -\frac{9N}{2us^2}(\lambda u + w - c_1), \tag{24}$$

$$s' = -\frac{M\theta}{3su}, \tag{25}$$

$$((c_1 - w)\theta)' = \Gamma\theta'' + \frac{RM\theta w}{us^2}, \tag{26}$$

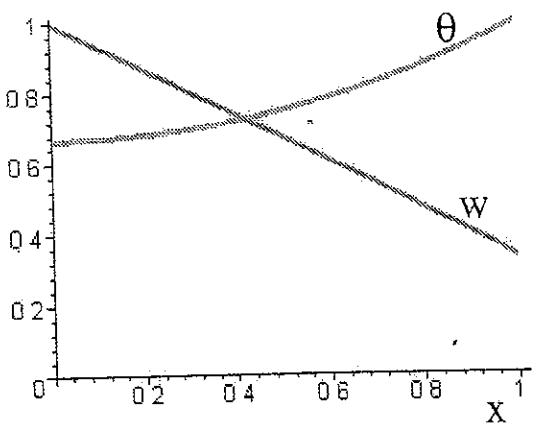


Figure 2: *Droplet size distribution and temperature as functions of non-dimensional distance for the case* $R = 4/10$, $M = \Gamma = 1$. *Here* $c_1 \simeq 0.35$, $c_2 \simeq 0.83$ *and there is no vapour layer*

with

$$s(0) = 1, \quad u(0) = 1, \quad \theta'(0) = 0, \quad w(0) = 0, \quad \theta(1) = 1, \quad w(1) = c_1. \tag{27}$$

Now (23) and (25) imply that

$$w = s^3$$

since $w = 1$ at $s = 1$, so that

$$w^{-1/3}w' = -\frac{M\theta}{u}, \tag{28}$$

$$uw^{2/3}u' = -\frac{9N}{2}(\lambda u + w - c_1) \tag{29}$$

and, using (23), (26) integrates to

$$\Gamma\theta' = (c_1 - w)\theta - Rw + c_2 \tag{30}$$

where $c_2$ is another constant. The three first–order equations (28)–(30) must be solved and $c_1$, $c_2$ determined using the five conditions (27).

It is only possible to make meaningful further analytic progress in the case $N = 0$, when the system reduces to the first–order equation

$$\Gamma\frac{d\theta}{dw} = \frac{\theta(w - c_1) + Rw - c_2}{M\theta w^{1/3}}$$

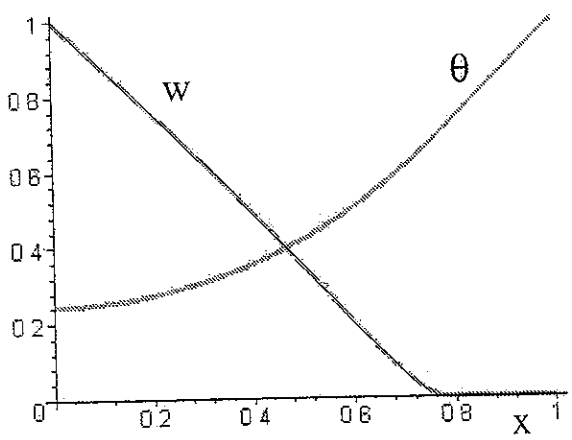


Figure 3: *Droplet size distribution and temperature as functions of non-dimensional distance for the case* $R = 4/10$, $M = 5$ *and* $\Gamma = 1/2$ *Here* $c_1 = 0$, $c_2 \simeq 0\,646$ *and a vapour layer exists in the region* $\ell \simeq 0.772 \leq x \leq 1$

with

$$w(0) = 1, \quad \theta(0) = \frac{R - c_2}{c_1 - 1}$$

and

$$w(1) = c_1, \quad \theta(1) = 1.$$

It is now relatively easy to find $\theta$, $w$, $c_1$ and $c_2$ by numerical integration; we therefore present some illustrative numerical results

When $R = 4/10$ and $M = \Gamma = 1$, we find that $c_1 \simeq 0\ 35$, $c_2 \simeq 0.83$ and the droplet size distribution and temperature are as shown in Figure 2: since $c_1 > 0$ there is no "dry-out", i.e. no droplet-free vapour layer near to the steel.

However, when we set $R = 4/10$, $M = 5$ and $\Gamma = 1/2$ we find that $c_1 = 0$ so that the droplets evaporate before they reach the steel at a position $\ell \simeq 0.772$ (with $c_2 \simeq 0\ 646$). The results in this case are shown in Figure 3; the value of $\ell$ is determined by requiring that $\theta$ be continuous at $x = \ell$ and that a layer of pure vapour exists in $\ell \leq x \leq 1$

Various asymptotic limits may also be considered. For example, when $M \gg 1$ and $M\Gamma = O(1)$, the solution is given by $c_2 = 0$ and $\theta = 0$, $w = 1$ except in a boundary layer near to $x = 1$. In this boundary layer $w = O(1)$, $\theta = \phi(\xi)/(M\Gamma)$ and $x = \ell - \xi\sqrt{\Gamma/M}$ where $0 \leq \xi < \infty$ is the boundary layer variable and $\phi$ denotes the temperature in the boundary layer Though the boundary layer equations cannot be solved in closed form, since $\theta' = c_2/\Gamma$ for $\ell \leq x \leq 1$ we have

$$\ell = 1 - \frac{\Gamma}{R}\left(1 - \frac{\phi(0)}{\sqrt{M\Gamma}}\right)$$

so that the vapour layer is thin. Numerical results for the case $M = 40$, $\Gamma = 1/40$ and $R = 4/10$ are shown in Figure 4. Here $\ell \simeq 0.982$, $c_2 \simeq 0\ 400002$, and the boundary layer scalings are thus corroborated.

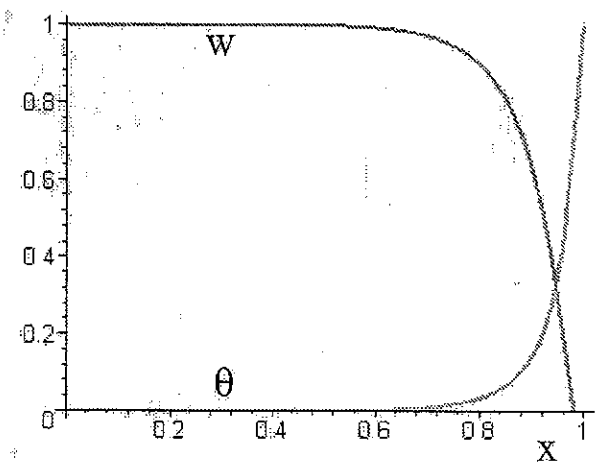


Figure 4: *Droplet size distribution and temperature as functions of non-dimensional distance for the case* $R = 4/10$, $M = 40$ *and* $\Gamma = 1/40$. *Here* $c_1 = 0$, $c_2 \simeq 0.400002$ *and a vapour boundary layer exists in the region* $\ell \simeq 0.982 \leq x \leq 1$

In the limit $M \gg 1$, $\Gamma M \gg 1$ it is possible to derive a closed form solution to the boundary layer problem, though this is too complicated to be helpful. Other asymptotic limits may also be examined, but we do not pursue them further here. However, these simple numerical experiments suggest that the model (23)–(27) can be used as a design tool to determine conditions under which dry-out occurs

### 2.5 Comments and conclusions

The above modelling and analysis neglects many aspects of spray cooling, both physical and mathematical. On the modelling side, we have ignored the implications of droplet size distribution, the discrete nature of the spray heads, compressibility effects and the presence of an air/steam mixture On the numerical side, our numerical results have given us confidence that the model as proposed can predict dry-out and hence be used to give quantitative information about controlling the cooling so that dry-out occurs just at the steel surface. This is likely to be the optimal operating regime, in which the maximum cooling is obtained for a given water supply.

## 3 Blast Furnace Reaction fronts

### 3.1 Physical Background

A typical blast furnace is shown in Figure 5. Its function is to produce pig iron from raw materials including iron ore, coke and limestone. These granular solids descend continuously through the furnace at the same time as air moves up through the granular structure having been preheated to 1000°C and blasted in through the tuyeres at the base of the furnace. This causes the coke to burn in a reaction zone, and the resulting liquid slag and pig iron collect at the bottom of the furnace.

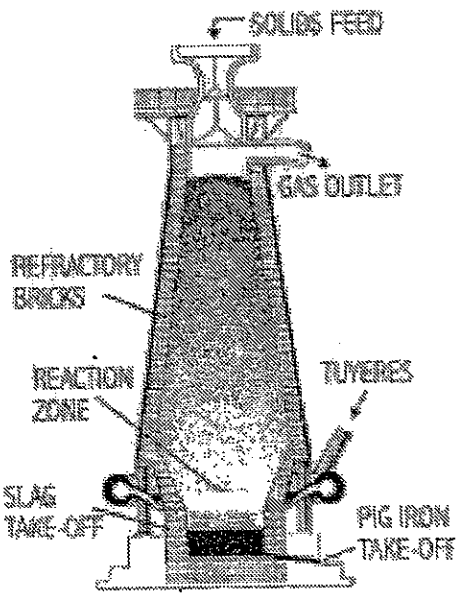


Figure 5: *General details of a typical blast furnace*

There are many aspects of blast furnace operation that warrant mathematical modelling (see, for example, [7]), but here we will focus on the reaction zone, traditionally referred to as the "intermediate region" (IR). This is a relatively thin layer at the base of the solids, whose geometry has been found to be a key indicator of the performance of the furnace. In particular, the locations of the maxima and minima of the height of the IR have been proposed as parameters that should be used to control furnace operation. Hence the ultimate aim of the mathematical modelling is to understand the relationship between the shape of the IR and the pig iron production rate, and we will attempt to do this by formulating a free boundary model for the IR.

### 3.2 One-dimensional Heat and Mass Transfer

We begin by proposing a simple one-dimensional heat transfer model to determine the location of the intermediate region in a blast furnace operated continuously in a steady state

A schematic diagram of the geometry and nomenclature that has been adopted is given in Figure 6 Under the assumptions listed below, the equations for the variables $T_s$, $T_g$, $u_g$ and $p_g$ are as follows:

$$\alpha_s \rho_s c_s u_s T_{sx} = h(T_g - T_s), \tag{31}$$

$$\alpha_g \rho_g c_g u_g T_{gx} = h(T_s - T_g), \tag{32}$$

$$u_{gx} = 0, \tag{33}$$

$$u_g \mid u_g \mid = -K p_{gx}, \tag{34}$$

where the subscripts $g$ and $s$ refer to the gas and solid phases respectively, $T$ denotes temperature, $\rho$ denotes density, $c$ denotes specific heat, $\alpha$ denotes volume fraction ($\alpha_s + \alpha_g = 1$), $u$ denotes speed, $p$ denotes pressure, $K$ is a (positive) constant with dimensions $m^4/kg$ and the subscript $x$ denotes differentiation in the vertical direction. The quantity $h > 0$ is a heat transfer coefficient that is assumed to be known and has dimensions $W/m^3/K$. The solids are descending, so that $u_s < 0$ and the gas ascends, so that $u_g > 0$.

The boundary conditions for (31)–(34) are taken to be

$$T_s(L) = T_a, \quad p_g(L) = p_a \tag{35}$$

and, at the free boundary $x = d$,

$$T_g(d) = T_{g0} + T_a, \quad p_g(d) = p_{g0} + p_a, \quad T_s(d) = T_m - \frac{\Delta H \alpha_c}{\rho_s c_s}. \tag{36}$$

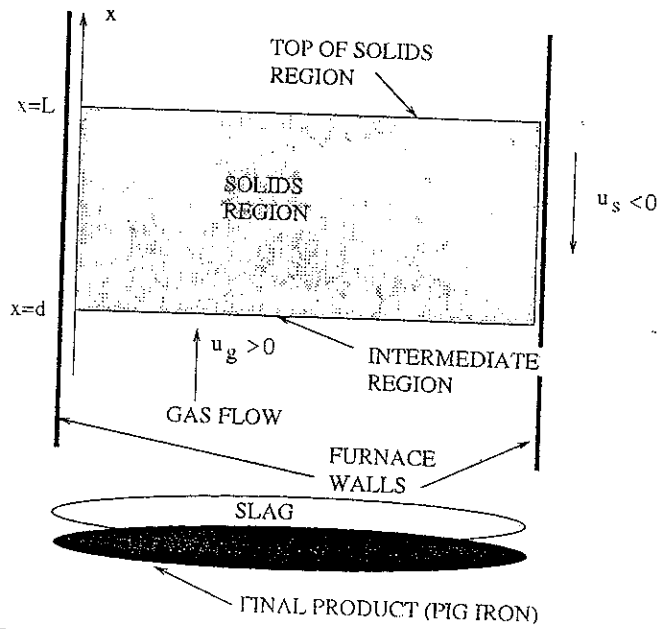


Figure 6: *Schematic and nomenclature for mathematical.*

Here $x = L$ denotes the top of the solids region in the furnace and $x = d(< L)$ denotes the unknown location of the intermediate region. $T_a$ and $p_a$ are respectively the temperature and pressure at the top of the furnace, $T_{g0}$ and $p_{g0}$ respectively are the excess temperature and pressure over ambient at which the hot gas is injected through the tuyeres, $\alpha_c < \alpha_s$ is the volume fraction of coal/coke in the solid phase, $\Delta H$ is the heat of reaction and $T_m$ denotes the temperature at which the ore is converted into liquid pig iron; typical values of all of these parameters are listed in the Appendix 2.

The equations and boundary conditions (31)–(36) include many modelling assumptions. These may be summarised as follows·

- Only thermal energy is considered and, above the reaction region, energy is conserved in both the gas and the porous solid phase, there being no heat transfer through the furnace walls. Energy is transferred from the gas to the solid and *vice versa* via a heat transfer coefficient $h$.

- Heat conduction is ignored in both equations (31) and (32). This is justifiable since, using the values in Appendix 2, the thermal conductivities $k_s$ and $k_g$ are such that

$$\frac{k_s}{\rho_s c_s(-u_s)L} \sim 0.0025, \qquad \frac{k_g}{\rho_g c_g u_g L} \sim 2\,2 \times 10^{-6}.$$

- For simplicity we assume that the $u_s$ is known from measurements, and that, because of constant replenishment with solids, the top of the solids region $x = L$ is fixed.

- Ergun's law [2] is assumed to apply in the solids region. This means that the superficial gas flow velocity $u_g$ (i.e. the velocity measured by the total gas mass flow through the furnace) is given by

$$\frac{\Delta P}{L} = \frac{150\mu_g(1-\alpha_g)u_g}{\alpha_g^3 a_p^2} + \frac{175(1-\alpha_g)\rho_g u_g \mid u_g \mid}{\alpha_g^3 a_p}$$

  where $L$ is the length of the region across which a pressure drop $\Delta P$ is applied, $\mu_g$ is the fluid dynamic viscosity and $a_p$ the diameter of a typical solid particle. In this formula, the first of the terms on the right-hand side may be thought of as representing the "Darcy" contribution to the flow, while the second represents the effects of inertia. Using the values in Appendix 2, we find that the ratio of the former to the latter term is approximately $4 \times 10^{-3}$, and thus the Darcy contribution has henceforth been ignored.

- We have assumed that pig iron production takes place only in the intermediate region and that consequently no molten iron drips down through the porous medium from above the intermediate region. Additionally, we have assumed that the latent heat of the melting of the iron at the intermediate region may be lumped into the reaction

- All chemical reactions have been ignored except in the last boundary condition (36). This may be derived by considering the combined effects of heat conduction and an exothermic reaction in the IR (see, for example,[8])

### 3.3 Non-dimensional Equations and Parameter Identification

Since one of our main reasons for proposing a simple model of a blast furnace is to identify suitable control parameters, we now non-dimensionalise (31)–(36). The length scale is chosen naturally so that gas-solid heat transfer balances convection; we thus scale using

$$x = L + \left(\frac{\alpha_s \rho_s c_s u_s}{h}\right)\bar{x}$$

and

$$T_s = T_a + (T_m - T_a)\bar{T}_s, \quad T_g = T_a + (T_m - T_a)\bar{T}_g,$$
$$p_g = p_a + p_{g0}\bar{p}_g, \quad u_g = -U\bar{u}_g, \tag{37}$$

where

$$U = \sqrt{\frac{-p_{g0}hK}{\alpha_s\rho_s c_s u_s}}$$

and an overbar denotes a non-dimensional quantity After non-dimensionalisation, the problem is defined on the region $0 \leq \bar{x} \leq \bar{d}$ where

$$\bar{d} = \frac{(d-L)h}{\alpha_s\rho_s c_s u_s} > 0,$$

and it is important to note that the intermediate region is now "above" the top of the solids which are at $\bar{x} = 0$ The non-dimensional governing equations become

$$\begin{aligned} \bar{T}_{s\bar{x}} &= \bar{T}_g - \bar{T}_s, \\ \beta\bar{u}_g\bar{T}_{g\bar{x}} &= \bar{T}_s - \bar{T}_g, \\ \bar{u}_{g\bar{x}} &= 0, \\ \bar{u}_g &= -\mid \bar{p}_{g\bar{x}} \mid^{-1/2} \bar{p}_{g\bar{x}}, \end{aligned}$$

and the non-dimensional boundary conditions are

$$\bar{T}_s(0) = 0, \quad \bar{p}_g(0) = 0$$

and

$$\bar{T}_g(\bar{d}) = \gamma, \quad \bar{p}_g(\bar{d}) = 1, \quad \bar{T}_s(\bar{d}) = 1 - \delta.$$

The key non-dimensional positive parameters $\beta$, $\gamma$ and $\delta$ are defined by

$$\beta = \frac{\alpha_g\rho_g c_g U}{\alpha_s\rho_s c_s(-u_s)}, \quad \gamma = \frac{T_{g0}}{T_m - T_a}, \quad \delta = \frac{\triangle H\alpha_c}{\rho_s c_s(T_m - T_a)}.$$

Though the physically obvious control parameters in the problem are the initial gas temperature $T_{g0}$, the initial gas pressure $p_{g0}$, the chemical "mix" of the solids (represented in our model by $\triangle H$ and $\alpha_c$) and the material replenishment rate at the top of the furnace, in our model the process is controlled only by the three non-dimensional parameters $\beta$, $\gamma$ and $\delta$ Using the values in Appendix 2, we find that

$$\beta \sim 6, \quad \gamma \sim 0\,7, \quad \delta \sim 0\,01, \tag{38}$$

but further investigation of some of the key parameters may be required before we can be sure of the orders of magnitude suggested by (38)

The equations may now be solved using elementary methods. We find that

$$\bar{u}_g = -(\bar{d})^{-1/2}, \quad \bar{p}_g = \frac{\bar{x}}{\bar{d}} \tag{39}$$

and, assuming that $\beta\bar{u}_g + e^{-\theta\bar{d}} \neq 0$, the temperatures are given by

$$\bar{T}_s = \frac{\gamma\beta\bar{u}_g(1 - e^{-\theta\bar{x}})}{\beta\bar{u}_g + e^{-\theta\bar{d}}}, \quad \bar{T}_g = \frac{\gamma(\beta\bar{u}_g + e^{-\theta\bar{x}})}{\beta\bar{u}_g + e^{-\theta\bar{d}}}, \tag{40}$$

where we have written

$$\theta = 1 + \frac{1}{\beta\bar{u}_g}$$

Imposing the final boundary condition that $\bar{T}_s(\bar{d}) = 1 - \delta$ now gives a transcendental equation for the non-dimensional position of the intermediate region $\bar{d}$ in the form

$$1 - \delta = \frac{\gamma\beta\bar{u}_g(1 - e^{-\theta\bar{d}})}{\beta\bar{u}_g + e^{-\theta\bar{d}}}. \tag{41}$$

This may be rewritten as

$$\frac{1-\delta}{\gamma} = f(\bar{d};\beta) \tag{42}$$

where

$$f(\bar{d};\beta) = \frac{\beta[1 - \exp(-\bar{d}(1 - \sqrt{\bar{d}}/\beta))]}{\beta - \sqrt{\bar{d}}\exp(-\bar{d}(1 - \sqrt{\bar{d}}/\beta))}.$$

We note immediately that only two combinations of the control parameters ($\beta$ and $(1-\delta)/\gamma$) determine the location of $\bar{d}$. Analysis of $f(\bar{d};\beta)$ further shows that $f(0;\beta) = 0$ and $f \to 0$ as $\bar{d} \to \infty$. A sketch of a typical $f(\bar{d};\beta)$ vs $\bar{d}$ curve is shown in Figure 7 for the illustrative value $\beta = 1$. The function $f$ has a single maximum which must be determined numerically (except for the special case when $\bar{d} = \beta^2$; see below). Denoting the maximum of $f$ for a given value of $\beta$ by $f_\beta$, we conclude that $\bar{d}$ exists (though it is non-uniquely determined) unless

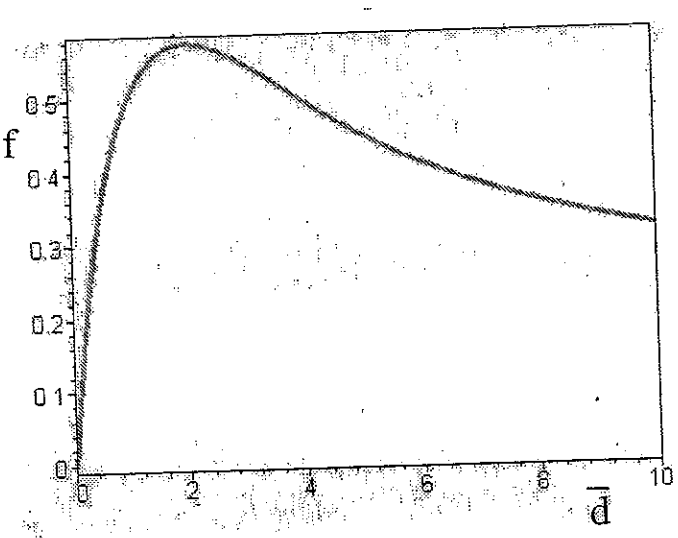


Figure 7: $f(\bar{d};\beta)$ *vs.* $\bar{d}$ *for illustrative value* $\beta = 1$

$$\frac{1-\delta}{\gamma} > f_\beta.$$

This condition means that the problem has no solution when

$$1 - \frac{\triangle H\alpha_c}{\rho_s c_s(T_m - T_a)} > \frac{T_{g0}f_\beta}{T_m - T_a}$$

i.e. when

$$f_\beta\rho_s c_s T_{g0} + \triangle H\alpha_c < \rho_s c_s(T_m - T_a)$$

This appears to be sensible on physical grounds as it asserts that no solution to the problem is possible if $T_m$ is too large (the reaction happens at too high a temperature), if $T_{g0}$ is too small (the gas in the tuyeres is not hot enough), if $\triangle H$ is too small (not enough heat of reaction) or if $\alpha_c$ is too small (not enough fuel in the solids). We return to the issue of the non-uniqueness of the position of the intermediate region in section 3.5.

It has been implicitly assumed that $\bar{d} \neq \beta^2$ in (41). This restriction arises from the fact that there is one special case; if it happens that

$$\frac{1-\delta}{\gamma} = \frac{\beta^2}{1+\beta^2}$$

then the solution is given simply by

$$\bar{T}_g = \frac{\gamma(1+\bar{x})}{1+\beta^2}, \quad \bar{T}_s = \frac{\gamma\bar{x}}{1+\beta^2}, \quad \bar{p}_g = \frac{\bar{x}}{\bar{d}},$$

$$\bar{u}_g = -\frac{1}{\sqrt{\bar{d}}}, \quad \bar{d} = \beta^2.$$

### 3.4 Two-dimensional Heat and Mass Transfer

It is a matter of great interest to study possible lateral variations in the location of the intermediate region. To study these, we assume that the blast furnace has width $2w$ and the extent of the solids region is $\{R : d(y) \leq x \leq L, \ -w \leq y \leq w\}$. We ignore conduction across the furnace which means that it will not be possible to impose temperature boundary conditions on the furnace wall. We also assume that, although the gas may flow in both the $x$- and the $y$-directions and has velocity $\boldsymbol{q}_g = u_g\boldsymbol{e}_x + v_g\boldsymbol{e}_y$ (where $\boldsymbol{e}_x$ and $\boldsymbol{e}_y$ are unit vectors in the $x$ and $y$ directions respectively), the velocity of the solids is still given by $\boldsymbol{q}_s = u_s\boldsymbol{e}_x$ with $u_s < 0$ prescribed. The steady-state governing equations are now

$$\alpha_s\rho_s c_s u_s T_{sx} = h(T_g - T_s),$$

$$\alpha_g\rho_g c_g[u_g T_{gx} + v_g T_{gy}] = h(T_s - T_g),$$

$$u_{gx} + v_{gy} = 0,$$

$$u_g = -\frac{Kp_{gx}}{\sqrt{u_g^2+v_g^2}}, \quad v_g = -\frac{Kp_{gy}}{\sqrt{u_g^2+v_g^2}},$$

with associated boundary conditions

$$T_s(L,y) = T_a, \quad p_g(L,y) = p_a,$$

$$T_g(d,y) = T_{g0}(y) + T_a, \quad p_g(d,y) = p_{g0}(y) + p_a, \quad T_s(d,y) = T_m - \frac{\triangle H\alpha_c}{\rho_s c_s},$$

$$p_{gy}(x,\pm w) = 0,$$

since there is no gas flow thorough the furnace walls. We non-dimensionalise the problem, using (37) and

$$y = \left(\frac{\alpha_s\rho_s c_s u_s}{h}\right)\bar{y}, \quad v_g = -U\bar{v}_g,$$

where, as before,

$$U = \sqrt{\frac{-p_{g0}hK}{\alpha_s\rho_s c_s u_s}}.$$

The equations then become

$$\begin{aligned} \bar{T}_{s\bar{x}} &= \bar{T}_g - \bar{T}_s, \\ \beta[\bar{u}_g \bar{T}_{g\bar{x}} + \bar{v}_g \bar{T}_{g\bar{y}}] &= \bar{T}_s - \bar{T}_g, \\ \bar{u}_{g\bar{x}} + \bar{v}_{g\bar{y}} &= 0, \\ \bar{q}_g &= -\frac{1}{|\, q_g \,|} \bar{\nabla} \bar{p}_g, \end{aligned}$$

with associated boundary conditions

$$\bar{T}_s(0,\bar{y}) = 0, \quad \bar{T}_g(\bar{d},\bar{y}) = \frac{T_{g0}(\bar{y})}{T_m - T_a}, \quad \bar{T}_s(\bar{d},\bar{y}) = 1-\delta, \tag{43}$$

$$\bar{p}_g(0,\bar{y}) = 0, \quad \bar{p}_g(\bar{d},\bar{y}) = \frac{p_{g0}(\bar{y})}{p_{g0}}, \quad \bar{p}_{g\bar{y}}(\bar{x},\pm\bar{w}) = 0 \tag{44}$$

where

$$\bar{d} = \frac{(d-L)h}{\alpha_s \rho_s c_s u_s}, \quad \bar{w} = \frac{wh}{\alpha_s \rho_s c_s u_s}.$$

Noting that

$$\bar{u}_g^2 + \bar{v}_g^2 = \frac{\bar{p}_{g\bar{x}}^2 + \bar{p}_{g\bar{y}}^2}{\bar{u}_g^2 + \bar{v}_g^2},$$

we find that the governing equation for $\bar{p}_g$ is

$$\left( \frac{\bar{p}_{g\bar{x}}}{|\, \bar{\nabla} \bar{p}_g \,|^{1/2}} \right)_{\bar{x}} + \left( \frac{\bar{p}_{g\bar{y}}}{|\, \bar{\nabla} \bar{p}_g \,|^{1/2}} \right)_{\bar{y}} = 0. \tag{45}$$

There is clearly little hope of finding exact solutions to (45) for a general unknown boundary $\bar{d}$ and even its numerical solution is non-trivial. However, we can use (45) to examine the the stability of the one-dimensional solution (40).

### 3.5 One-dimensional Stability

It is natural to investigate the temporal stability of the solution (40). Adding time variations to the heat transfer equations and non-dimensionalising time using $t = (\alpha_s \rho_s c_s / h)\bar{t}$, the non-dimensional problem that must now be solved is

$$\bar{T}_{s\bar{t}} + \bar{T}_{s\bar{x}} = \bar{T}_g - \bar{T}_s, \tag{46}$$

$$\left( \frac{\alpha_g \rho_g c_g}{\alpha_s \rho_s c_s} \right) \bar{T}_{g\bar{t}} + \beta \bar{u}_g \bar{T}_{g\bar{x}} = \bar{T}_s - \bar{T}_g, \tag{47}$$

$$\bar{u}_{g\bar{x}} = 0, \tag{48}$$

$$\bar{u}_g \,|\, \bar{u}_g \,| = -\bar{p}_{g\bar{x}}, \tag{49}$$

with associated boundary conditions

$$\bar{T}_s(0) = 0, \quad \bar{p}_g(0) = 0, \quad \bar{T}_g(\bar{d}) = \gamma, \quad \bar{p}_g(\bar{d}) = 1, \quad \bar{T}_s(\bar{d}) = 1-\delta.$$

Using the values in Appendix 2, it transpires that the gas temperature parameter $(\alpha_g \rho_g c_g)/(\alpha_s \rho_s c_s)$ is negligible and we shall therefore ignore the time derivative in (47). For the remainder of this

section the overbars will be dropped for convenience We deal with the Ergun equation first, and set

$$u_g = u_{g0} + \epsilon Re(u_{g1}e^{\sigma t}) + ..., \quad p_g = p_{g0} + \epsilon Re(p_{g1}e^{\sigma t}) + ... . \tag{50}$$

The free boundary is assumed to be at

$$x = d_0 + \epsilon Re(d_1 e^{\sigma t}) + ...,$$

where, as usual for linear stability analysis, $\epsilon$ is assumed to be "small" and $u_{g1}$, $p_{g1}$, $d_1$ and $\sigma$ are in general complex. On solving (48) and (49) and imposing the necessary conditions on the free boundary, we find that, as before,

$$u_{g0} = -\frac{1}{\sqrt{d_0}}, \quad p_{g0} = \frac{x}{d_0}$$

while

$$u_{g1} = \frac{d_1}{2d_0^{3/2}}, \quad p_{g1} = -\frac{d_1 x}{d_0^2}$$

We now turn to the heat transfer equations (46) and (47). We set

$$T_s = T_{s0} + \epsilon Re(T_{s1}e^{\sigma t}) + ...., \quad T_g = T_{g0} + \epsilon Re(T_{g1}e^{\sigma t}) + ... . \tag{51}$$

The leading order problem gives, as we already know,

$$T_{s0} = \frac{\gamma(1 - e^{-x(1-\phi)})}{1 - \phi e^{-d_0(1-\phi)}}, \quad T_{g0} = \frac{\gamma(1 - \phi e^{-x(1-\phi)})}{1 - \phi e^{-d_0(1-\phi)}},$$

where

$$\phi = \frac{\sqrt{d_0}}{\beta}.$$

The $O(\epsilon)$ problems for the temperature perturbations are

$$(1 + \sigma)T_{s1} - T_{g1} + T'_{s1} = 0$$

$$T_{g1} - T_{s1} - \frac{1}{\phi}T'_{g1} + \frac{d_1\gamma(1-\phi)e^{-x(1-\phi)}}{2d_0[1 - \phi e^{-d_0(1-\phi)}]} = 0$$

where a dash denotes a derivative with respect to $x$. On elimination of $T_{g1}$, we find that

$$\sigma T_{s1} + \left[1 - \frac{(1+\sigma)}{\phi}\right]T'_{s1} - \frac{1}{\phi}T''_{s1} = \frac{d_1\gamma(\phi-1)e^{-x(1-\phi)}}{2d_0[1 - \phi e^{-d_0(1-\phi)}]} \tag{52}$$

At the free boundary we require $T_s = 1 - \delta$. This gives one boundary condition for $T_s$ in the form

$$T_{s1}(d_0) = -\frac{\gamma d_1(1-\phi)e^{-d_0(1-\phi)}}{1 - \phi e^{-d_0(1-\phi)}}, \tag{53}$$

and another is evidently $T_{s1}(0) = 0$. We note also that $T_g(d) = \gamma$, and expanding this at the free boundary gives

$$T_{g1}(d_0) = -\frac{\gamma\phi d_1(1-\phi)e^{-d_0(1-\phi)}}{1 - \phi e^{-d_0(1-\phi)}}$$

(which we note is also equal to $\phi T_{s1}(d_0)$). We may now use the fact that

$$T_{g1} = (1+\sigma)T_{s1} + T'_{s1}$$

to see that

$$(1+\sigma-\phi)T_{s1}(d_0) + T'_{s1}(d_0) = 0. \tag{54}$$

We may now find $T_{s1}$ from (52). By elementary methods, it may be shown that

$$T_{s1} = C_1 e^{k^+ x} + C_2 e^{k^- x} - \frac{d_1\gamma\phi(1-\phi)e^{-x(1-\phi)}}{2\sigma d_0[1-\phi e^{-d_0(1-\phi)}]},$$

where $C_1$ and $C_2$ are arbitrary constants and

$$k^{\pm} = \frac{\phi - 1 - \sigma \pm \sqrt{(\phi-1-\sigma)^2 + 4\sigma\phi}}{2}.$$

If we now impose the boundary conditions $T_{s1}(0) = 0$ and (53), we find eventually that

$$T_{s1} = \frac{[d_1\gamma(1-\phi)(\phi-2\sigma d_0)e^{-d_0(1-\phi)} - d_1\gamma\phi(1-\phi)e^{d_0k^-}][e^{k^+x} - e^{k^-x}]}{2\sigma d_0[1-\phi e^{-d_0(1-\phi)}][e^{d_0k^+} - e^{d_0k^-}]} +$$

$$\frac{d_1\gamma\phi(1-\phi)(e^{k^-x} - e^{-x(1-\phi)})}{2\sigma d_0[1-\phi e^{-d_0(1-\phi)}]}.$$

Finally (54) becomes

$$(K^+ - K^-)[\phi^2 - \phi(1+2d_0\sigma) + 2\sigma d_0(1+\sigma)] + (k^+K^+ - k^-K^-)(2\sigma d_0 - \phi) +$$

$$(k^+ - k^-)\phi e^{-d_0\sigma} = 0 \tag{55}$$

where we have written

$$K^+ = e^{d_0k^+}, \quad K^- = e^{d_0k^-}.$$

Our task is now to solve (55) for $\sigma$ and examine whether there exist $\sigma$ with with real parts greater than zero, leading to instability.

### 3.6 Results of stability analysis

It is not difficult to solve (55) numerically. We find that, when the ratio $(1-\delta)/\gamma$ is small enough so that two values of $\bar{d}$ exist, in every case the smaller value is stable, whilst the larger one is unstable.

Though we have not been able to prove that all solutions of (55) are pure real, in every case that we have examined we have found only pure real roots. The following numerical results are typical of our findings: when $\beta = 1/3$ and $(1-\delta)/\gamma = 1/4$, we find from (42) that the two possible values for $\bar{d}$ are given by

$$\bar{d}_1 = 0.3950273496, \quad \bar{d}_2 = 1.7640150539$$

(Note that we have worked here to 10 decimal places; such accuracy is required if the values for $\sigma$ are to be determined with any confidence.) Corresponding to $\bar{d}_1$, we find the solutions

$$\sigma = -0.1392395948, \quad -2.5909704874 \text{ and } -5\,6318324789.$$

However, the $\sigma$ corresponding to $\bar{d}_2$ are

$$\sigma = +0.2510589794, \quad -0.9922509619 \text{ and } -8.9767227449,$$

showing that the solution corresponding to $\bar{d}_2$ is unstable.

In each one of the many cases that we examined, there were three purely real negative $\sigma$ corresponding to the smaller root $\bar{d}_1$, and just one pure real positive $\sigma$ and a number of pure real negative $\sigma$ corresponding to $\bar{d}_2$ We therefore conclude that the smaller value of $\bar{d}$ is the one that is likely to be observed in a real blast furnace.

### 3.7 Two-dimensional Stability

The methodology used in Section to study global one-dimensional stability becomes unmanageable when we consider two-dimensional disturbances to (40). Hence we confine attention to the stability of (40) to disturbances that are confined near the IR, i.e. that have wavelengths short compared to the size of the furnace. Hence (46)-(49) become, in non-dimensional form but with the overbars removed for convenience,

$$T_{st} + T_{sx} = T_g - T_s,$$

$$\beta(u_g T_{gx} + v_g T_{gy}) = T_s - T_g,$$

$$u_{gx} + v_{gy} = 0,$$

$$(u_g, v_g) = -\frac{1}{|\nabla p_g|^{1/2}} \nabla p_g.$$

We seek only unforced modes in which $T_{g0}$ and $p_{g0}$ are independent of $y$, so that, at the free boundary $x = d$, the conditions (43) and (44) are simply

$$T_g(d, y) = \gamma, \quad T_s(d, y) = 1 - \delta, \quad p_g(d, y) = 1.$$

For our local analysis, we need only the behaviour of (39) and (40) as $x \uparrow d_0$ Hence the solution about which we will perturb is

$$d = d_0, \quad T_{s0} = 1 - \delta + (\gamma + \delta - 1)(x - d_0), \quad T_{g0} = \gamma + \frac{\sqrt{d_0}}{\beta}(\gamma + \delta - 1)(x - d_0)$$

and

$$p_{g0} = 1 + \frac{1}{d_0}(x - d_0), \quad u_{g0} = -\frac{1}{\sqrt{d_0}},$$

with the requirement that the perturbations are small compared to this steady state as $x - d_0 \to -\infty$. When we proceed as in (50) and (51), we find that

$$\sigma T_{s1} + T_{s1x} = T_{g1} - T_{s1}, \tag{56}$$

$$\beta(u_{g0} T_{g1x} + T_{g0x} u_{g1}) = T_{s1} - T_{g1}, \tag{57}$$

$$u_{g1x} + v_{g1y} = 0$$

and

$$u_{g1} = -\frac{\sqrt{d_0}}{2} p_{g1x}, \quad v_{g1} = -\sqrt{d_0} p_{g1y}$$

At $x = d_0$, we need to satisfy

$$T_{g1} + \frac{\sqrt{d_0}}{\beta}(\delta + \gamma - 1)d_1 = 0,$$

$$T_{s1} + (\delta + \gamma - 1)d_1 = 0,$$

and

$$p_{g1} + \frac{d_1}{d_0} = 0. \tag{58}$$

Since $p_{g1xx} + 2p_{g1yy} = 0$ , we can now seek disturbances with real wavenumber $k$ in the form $p_{g1} \propto \exp(iky + \sqrt{2}k(x - d_0))$ where, without loss of generality, we assume that $k > 0$. From (58), with $d_1 = \tilde{d}_1 \exp(iky)$, we find that

$$p_{g1} = -\frac{\tilde{d}_1}{d_0}\exp(iky + \sqrt{2}k(x - d_0)), \quad u_{g_1} = \frac{k\tilde{d}_1}{\sqrt{2}d_0}\exp(iky + \sqrt{2}k(x - d_0)).$$

Hence, from (56) and (57) with

$$T_{s1} = \tilde{T}_s(x)\exp(iky), \quad T_{g1} = \tilde{T}_g(x)\exp(iky),$$

we have

$$-\frac{\beta}{\sqrt{d_0}}\tilde{T}_s'' + \left(1 - \frac{\beta}{\sqrt{d_0}}(1 + \sigma)\right)\tilde{T}_s' + \sigma\tilde{T}_s = -\frac{(\delta + \gamma - 1)k\tilde{d}_1}{\sqrt{2}}\exp(\sqrt{2}k(x - d_0))$$

with

$$\tilde{T}_g + \frac{\sqrt{d_0}}{\beta}(\delta + \gamma - 1)\tilde{d}_1 = 0$$

and

$$\tilde{T}_s + (\delta + \gamma - 1)\tilde{d}_1 = 0$$

at $x = d_0$, and

$$\sigma\tilde{T}_s + \tilde{T}_s' = \tilde{T}_g - \tilde{T}_s;$$

here $'$ denotes $d/dx$ and we also require decay as $x \to -\infty$. Once again writing $\phi = \sqrt{d_0}/\beta$ and denoting the roots of

$$-\frac{1}{\phi}r^2 + \left(1 - \frac{1}{\phi}(1 + \sigma)\right)r + \sigma = 0$$

by $r^{\pm}$, where the real part of $r^+$ is not less than the real part of $r^-$, we see that we cannot relate $\sigma$ and $k$ when the real parts of $r^{\pm}$ are equal. But if

$$\mathrm{Re}(r^+) > 0 > \mathrm{Re}(r^-), \tag{59}$$

then we can derive the dispersion relation

$$k^2[4(r^+ + \sigma + 1) - 6\phi] + k\sqrt{2}[2(\sigma - \phi)^2 + 4(\sigma - \phi) + 2 + r^+(2 + 2\sigma - \phi)]$$

$$-2\sigma\phi(\sigma - \phi + 1 + r^+) = 0. \tag{60}$$

Though the dispersion relation (60) appears at first to be a quartic equation for $\sigma$, further simplification shows that the $\sigma^4$ term cancels. As a consequence of this, (60) may be solved for $\sigma$ to yield the relatively simple expressions

$$\sigma = \frac{k(-2k - \sqrt{2} + \sqrt{2}\phi)}{\sqrt{2}k - \phi} \tag{61}$$

and

$$\sigma = \frac{Q \pm \sqrt{Q^2 - 2\sqrt{2}k(3k - \sqrt{2}\phi)(-2k + 3k\phi - \sqrt{2}(1-\phi)^2)}}{2(6k - 2\sqrt{2}\phi)} \tag{62}$$

where

$$Q = -2k\phi + 4k + 3\sqrt{2}k^2.$$

Further analysis requires more space than is available here. However, it may easily be shown that for $k \gg 1$, the three values of $\sigma$ in (61) and (62) for which (59) is satisfied are

$$\sigma \sim \frac{\phi}{2} - \frac{1}{3} + O(1/k),$$

$$\sigma \sim -\sqrt{2}k - \left(\frac{\phi}{2} + 1\right) + O(1/k)$$

and

$$\sigma \sim -\sqrt{2}k - 1 + O(1/k).$$

We therefore conclude that short wave disturbances are stable provided that $\phi < 2/3$, i.e. provided that $\sqrt{d_0} < 2\beta/3$. Physically, this suggests that for short waves to be stable the ratio $U/(-u_s)$ must be large enough, so that the solids must not move too fast.

For long waves with $k \ll 1$, we find that the three roots satisfy $\sigma \sim O(k)$ and

$$\sigma \sim \pm\sqrt{\frac{k(\phi-1)^2}{\phi\sqrt{2}}} + O(k);$$

long wavelength instabilities are thus inevitable.

## 4 Conclusions

We have derived, and given some preliminary analysis of two novel free boundary problems for fundamental processes in the steel industry. The first problem concerns spray cooling and it eventually leads to the novel dynamical system (28)–(30) whose singular behaviour determines the location of the of the vapour layer that controls the efficiency of the cooling. The second problem leads to an unconventional free boundary problem in a reacting porous medium, the free boundary being the all-important "intermediate region". Our stability analysis suggests that this model has many interesting features that await further attention.

## Acknowledgements

This research was carried out as a result of problems that were brought to the first and second Chinese Study Groups with Industry, held at Fudan University, Shanghai, P.R. China in September 2000 and November 2001. These meetings were supported by Royal Society Project Q791. The authors wish to thank the organisers of this meeting for help and inspiration, and in particular Professor Tan Yongji of the Department of Mathematics, Fudan University. The problems analysed here were originally posed by representatives from Linfen Steel and Bao Steel, and the authors are particularly grateful to Dr. Z. Guo from Bao Steel.

## References:

[1] Drew, D.A. & Passman, S.L. (1999) *Theory of Multicomponent Fluids*[M] (Applied Mathematical Sciences) New York: Springer-Verlag 330pp

[2] Ergun, S. (1952) Flow through packed columns[J]. Chem. Eng. Prog. **48**, 89–94.

[3] Chandra, S. & Aziz, S.D. (1994) Leidenfrost evaporation of liquid nitrogen droplets[J] Trans. ASME, J. Heat Transfer **116**, 999–1006.

[4] Ishii, M. & Zuber, M. (1979) Relative motion and interfacial drag coefficient in dispersed two-phase flow of bubbles, drops and particles[J]. A.I.Ch.E. J. **25**, 843–857.

[5] Kaye, G.W.C. & Laby, T.H. (1968) *Tables of Physical and Chemical Constants*[M] London: Longmans 223pp.

[6] Lide, D.R. (Ed.) (1997) *CRC Handbook of Chemistry and Physics*[M], *78th Edition* Ney York: CRC Press.

[7] McGannon, H.E. (Ed.) (1971) *The Making, Shaping and Treating of Steel, 9th Edn*[M]. Pittsburgh: United States Steel.

[8] Aldushin, A.P. & Matkowsky, B.J. (1998) Rapid filtration combustion waves driven by convection[J] Combust. Sci. Technol. **140**, 259–293

[9] *UK Steam Tables in SI Units*, (1970) London: Edward Arnold.

[10] Vasserman, A.A., Kazavchinskii, Ya. Z. & Rabinovich, V.A. (1971) *Thermophysical Properties of Air and Air Components* Jerusalem: Program for Soviet Translation.

## Appendix 1: typical values of constants used in spray cooling problem

There is by no means unanimity concerning the values of density, thermal conductivity and specific heat at high pressures and temperatures. In the current study though the temperatures may be as high as 1500°C, we do not expect pressures higher than a few bar as the system is not confined in any way. We have therefore used values from standard steam tables. Although these may not be completely accurate, they are unlikely to be in error by orders of magnitude. Data items marked with a dagger (†) are informed guesses on our part and need to be confirmed with Bao and/or Linfen steel.

$c_p = 4.214 \times 10^3 \mathrm{J/kg/K}$ (water, 10 bar, 100°C) ([9], p.116)

$c_{pg} = 2.032 \times 10^3 \mathrm{J/kg/K}$ (steam, 1 bar, 100°C)([9], p.116)

$k = 0.670 \mathrm{W/m/K}$ (water, 10 bar, 80°C)([9], p.124)

$k_g = 2.48 \times 10^{-2} \mathrm{W/m/K}$ (steam, 1 bar, 100°C) ([9], p.124)

$k_g = 1.35 \times 10^{-1} \mathrm{W/m/K}$ (steam, 1 bar, 1000°C) ([9], p.124)

$L = 2.257 \times 10^6 \mathrm{J/kg}$ (water, 100°C)([5], p.174)

$\mu_g = 1.81 \times 10^{-5} \mathrm{kg/m/s}$ (air, 1 bar, 20°C†)

$\rho_d = 958.5 \mathrm{kg/m^3}$ (water, 1 bar, 80°C)([9], p. 132)

$\rho_g = 0.590\text{kg/m}^3$ (steam, 1 bar, 100°C)([9], p. 132)
$\rho_g = 0.202\text{kg/m}^3$ (steam, 1 bar, 800°C)([9], p. 132)
$s_0 = 10^{-5}\text{m}$ (drop radius†)
$T_s = 500 - 2000°\text{C}$ (varies along the steel†)
$T_V = 100°\text{C}$ (assuming pressure conditions close to atmospheric†)
$U = 5\text{m/s}$ (typical drop speed†)
$D = 1\text{m}$ (typical spray nozzle to steel distance†)

## Appendix 2: typical values of constants used in blast furnace problem

(In some cases the given physical constants, being somewhat hard to find, are not given at the correct temperatures. We do not anticipate that the correct values will be very different from those listed below, however )

$a_p = 5\text{mm}$ (particle size (radius) of solids: variable)
$\alpha_c \sim 0.4$ (may vary from furnace to furnace)
$\alpha_g \sim 0.3$ (depends on particle size)
$c_g = 1.189 \times 10^3\text{J/kg/K}$ (air, 1 bar, 1300K) ([10])
$c_s = 0.709 \times 10^3\text{J/kg/K}$ (carbon (graphite), 1 bar, 300K) ([6])
$h \sim 10^{-4}\text{J/(m}^3\text{sec K)}$ (may be unreliable)
$\triangle H = 200\text{MJ/mol}$ (typical reaction; may be unreliable)
$K = 3.16 \times 10^5$ (Ergun constant: calculated from other values)
$k_g = 0.09\text{W/m/K}$ (air, 1 bar, 1400K) ([5])
$k_s = 40.0\text{W/m/K}$ (air, 1 bar, 293K) ([5])
$L = 10\text{m}$ (typical solids layer height)
$\nu_g = 2.5 \times 10^{-4}\text{m}^2\text{/sec}$ (air, 1 bar, 1600K)
$p_{g0} = 10^5$ Pa (1 bar)
$\rho_g = 0.348\text{kg/m}^3$ (air, 1 bar, 1000K) ([6])
$\rho_s = 7.8 \times 10^3\text{kg/m}^3$ (carbon steel) ([6])
$T_a = 30°\text{C}$ (typical ambient temperature)
$T_{g0} = 1000°\text{C}$ ([7])
$T_m = 1500°\text{C}$ (typical reaction temperature)
$u_g \sim 10\text{m/sec}$
$u_s = -1\text{m/hr} = -2.78 \times 10^{-4}\text{m/sec}$
$V_w = 1670\text{m}^3$ (total furnace working volume) ([7])
$w_b = 7\text{m}$ (working section width: furnace bottom) ([7])
$w_t = 10\text{m}$ (working section width: furnace top) ([7])